

Probing Neutrino Magnetic Moments at Underground Detectors with Artificial Neutrino Sources

O. G. Miranda ^{a*} J. Segura ^{b†}, V. B. Semikoz ^c,
and J. W. F. Valle ^{d‡}

^a *Departamento de Física
CINVESTAV-IPN, A. P. 14-740, México 07000, D. F., México.*

^b *Instituto de Bioingeniería
Universidad Miguel Hernández
Edificio La Galia
03202 Elche (Alicante) SPAIN*

^c *The Institute of the Terrestrial Magnetism,
the Ionosphere and Radio Wave Propagation of the Russian Academy of Science,
IZMIRAN, Troitsk, Moscow region, 142092, Russia*

^d *Instituto de Física Corpuscular - C.S.I.C.
Departament de Física Teòrica, Universitat de València
46100 Burjassot, València, SPAIN
<http://neutrinos.uv.es>*

Abstract

Neutrino-electron scattering can be used to probe neutrino electromagnetic properties at low-threshold underground detectors with good angular and recoil electron energy resolution. We propose to do this using a number of artificial neutrino and anti-neutrino sources such as $^{51}\text{Cr}_{24}$ and $^{90}\text{Sr}-\text{Y}$. The neutrino flux is known to within one percent, in contrast to the reactor case and one can reach lower neutrino energies. For the $^{90}\text{Sr}-\text{Y}$ source we estimate that the signal expected for a neutrino magnetic moment of $\mu_\nu = 6 \times 10^{-11} \mu_B$ will be comparable to that expected in the SM and corresponds to a 30% enhancement in the total number of expected events.

pacsl3.15.+g 12.20.Fv 14.60.St 95.55.Vj

* E-mail: omr@fis.cinvestav.mx

† E-mail: segura@flamenco.ific.uv.es

‡ E-mail valle@flamenco.ific.uv.es

1 Introduction

Low-energy-threshold underground detectors with good angular and recoil electron energy resolution open a new window to probe the structure of the weak interaction and neutrino electromagnetic properties [1] [2] as a good alternative to what can be learned at reactor and accelerator experiments [1, 3]. We propose to do this using a number of artificial neutrino and anti-neutrino sources such as $^{51}\text{Cr}_{24}$ and $^{90}\text{Sr} - \text{Y}$. The neutrino flux is known to within a one percent accuracy, in contrast to the reactor case and one can reach lower neutrino energies.

Non-standard neutrino properties have been studied for several years, partly motivated by the solar neutrino problem. A possible explanation of this problem is related to a large neutrino magnetic moment [4]. Present constraints for the electron neutrino magnetic moment coming from reactor experiments gives $\mu_\nu = 1.8 \times 10^{-10} \mu_B$ [5]. The improvement of this bound in a new reactor experiment is the goal of the MUNU [6] experiment, now running.

The idea of using an artificial neutrino source (ANS) to search for a neutrino magnetic moment was first put forward by Vogel and Engel in Ref. [1]. This kind of sources have already been used to calibrate both GALLEX and SAGE experiments [7] and, recently, this idea has been considered by several experimental groups working in underground physics. The ANS have as an advantage that the uncertainties in the neutrino flux intensity are lower than in the case of reactor neutrinos and they have a small size, which makes them suitable for a deep underground experiment; they could be even surrounded by the detector as is the plan for the LAMA collaboration [8] that has as a goal the use of a ^{147}Pm anti-neutrino source with a one ton NaI detector in order to test for a neutrino magnetic moment in the region $10^{-11} \mu_B < \mu_\nu < 10^{-10} \mu_B$. The BOREXINO collaboration has also the possibility of searching for a neutrino magnetic moment in such a region using an ANS located at a distance of the order of 10 m [9, 10].

Here analyse the potential of these sources in testing the neutrino magnetic moment in a detector with both angular and recoil electron energy resolution. Such a study could be interesting for a detector like that in the HELLAZ proposal [11] that is planning to detect neutrinos through neutrino electron scattering with an energy threshold as low as 100 KeV and with an angular resolution of 35 mrad. These two characteristics could make HELLAZ proposal adequate for improving the limits on neutrino properties by using artificial neutrino sources. The only limitation HELLAZ could have in comparison with BOREXINO is the large mass the last experiment is planning (100 tones vs. 6 tones) although this might be solve with an adequate experimental set up; for example, if it were possible to surround the source with the detector to get the full 4π neutrino source of the source, although in this case oscillation could not be studied.

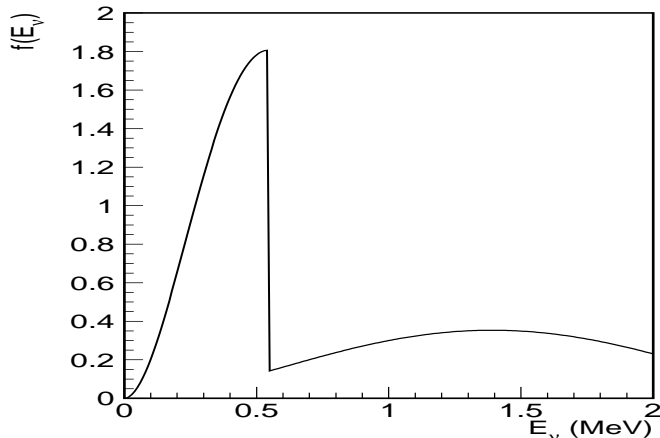


Figure 1: Sr-Y spectrum

2 Artificial Sources and Magnetic Moment

We will consider the next sources for being the most realistic and interesting ones in getting results:

- $^{51}\text{Cr}_{24}$ neutrino source. This is a neutrino source that has already been used for calibrating both SAGE and GALLEX experiments [7]. The main neutrino line is $E_\nu = 746$ KeV and the lifetime is 40 days.
- $^{49}\text{V}_{23}$ This is a neutrino source that produces neutrinos with energy $E_\nu = 602$ KeV. The lifetime is 1.3 years [12].
- $^{145}\text{Sm}_{62}$ This is a neutrino source that produces neutrinos with energy $E_\nu = 554$ KeV. The lifetime is 1.34 years [12].
- $^{37}\text{Ar}_{18}$ This is a neutrino source that produces neutrinos with energy $E_\nu = 814$ KeV. The lifetime is 35 days [12].
- ^{90}Sr anti-neutrino source. This source has been studied in Ref. [15] and its potential for the BOREXINO case has been already discussed [10]. The neutrino energy spectrum for such a source is shown in Fig 1. The half-life is 28 years.

For the case of neutrino sources the detectors which are now being proposed would be able to measure the differential cross section for the $\nu_e e$ scattering. At leading order in the SM this is given by

$$\frac{d\sigma^W}{dT} = \frac{2m_e G_F^2}{\pi} \left\{ g_L^2 + g_R^2 \left(1 - \frac{T}{E_\nu}\right)^2 - \frac{m_e}{E_\nu} g_R g_L \frac{T}{E_\nu} \right\} \quad (1)$$

where T is the recoil electron energy, and E_ν is the neutrino energy; $g_L = \frac{1}{2} + \sin^2\theta_W$ and $g_R = \sin^2\theta_W$.

For the case of an anti-neutrino source the process will be $\bar{\nu}_e - e$ scattering and we just need to exchange g_L with g_R in order to get the corresponding differential cross section.

On the other hand the differential cross section in the case of a neutrino magnetic moment is

$$\frac{d\sigma^{mm}}{dT} = \frac{\pi\alpha^2\mu_\nu^2}{m_e^2} \left\{ \frac{1}{T} - \frac{1}{E_\nu} \right\} \quad (2)$$

which adds incoherently to the weak cross section (neglecting neutrino mass).

It is well known from this equation that for lower values of T the neutrino magnetic moment signal will drastically increase. This makes interesting the use of low threshold detectors such as the one has been proposed by the HELLAZ collaboration, and which could reach a threshold as low as 100 KeV.

Besides the low energy threshold, HELLAZ will also have angular resolution. This could be useful not only to lower the systematic errors, but also to take advantage of the best regions in the (θ, T) plane where the non-standard effects could be bigger. Although the restriction to a narrow window will limit the statistics, the enhancement of the neutrino magnetic moment (NMM) effect may over-compensate and one might have an overall gain.

In [13] it was shown that $\frac{d\sigma^W}{dT}$ vanishes for forward electrons (which implies maximum recoil energy for e^-) for a $\bar{\nu}_e$ energy given by:

$$E_\nu = m_e \frac{g_L - g_R}{2g_R} = m_e/4\sin^2\theta_W \simeq 0.548MeV \quad (3)$$

This kind of cancellation only takes place when considering scattering of $\bar{\nu}_e$ off e^- . Of course, to be able to study this effect, experiments capable of measuring both the recoil (kinetic) energy of the electron (T) and its recoil angle (θ) become necessary, so that we can select neutrino energies E_ν from a non-monochromatic source (a monochromatic source of $\bar{\nu}_e$ with $E_\nu = m_e/4\sin^2\theta_W$ would be the ideal but there are not monochromatic anti-neutrino sources).

The three variables E_ν , T and θ are related by the equation:

$$\cos\theta = \frac{T}{\sqrt{T^2 + 2m_e T}} \left(1 + \frac{m_e}{E_\nu} \right) \quad (4)$$

As discussed in [13] the dynamical zero seems potentially interesting to measure μ_ν since it opens a window in phase space where the weak cross section becomes small, so that the magnetic moment contribution could eventually become larger than the weak cross section. However, as discussed in [14] in the context of reactor neutrino experiments, the fact that the statistics close to the dynamical zero is poor is, unfortunately, more important than the enhancement in $d\sigma^{mm}/d\sigma^W$.

2.1 Neutrino sources

We will consider first the case of a Cr neutrino source. As mentioned in the introduction this source has already been used for the calibration of SAGE and GALLEX

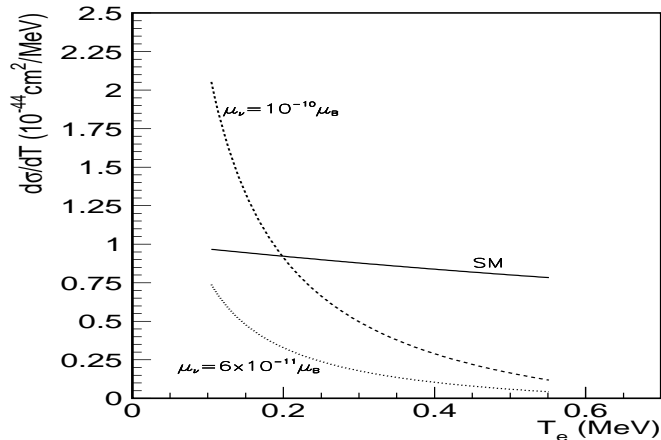


Figure 2: Differential cross section in terms of T for the SM case and for the neutrino magnetic moment contribution for two different values of μ_ν in the case of a Cr source.

experiments. We will consider the 746 KeV neutrino line that has the 81 % of the neutrino flux.

For this case the differential cross section will be as given in Eq. (1) and we just need to substitute the corresponding value for the neutrino energy. The result is shown in Fig 2 both for the Standard Model case as well as for the case of a neutrino magnetic moment. Different values of the magnetic moment are shown. As we can see, for low values of T the NMM signal is of the same order of the SM one for $\mu_\nu \sim .6 - 1 \times 10^{-10} \mu_B$.

The differential cross section

$$\frac{d\sigma^W}{d\cos\theta} = \frac{d\sigma^W}{dT} \frac{dT}{d\cos\theta} \quad (5)$$

can be easily obtained and it is shown in Fig. 3, where we can see a similar result: there is a region, for large electron recoil angle, for which the NMM signal is comparable to that of the SM. The similarities of these two figures are more evident if one notices that the recoil angle θ is maximum for lower T , as can be derived from Eq. (4).

For other neutrino sources different that the *Cr* source, the shape of the plots shown in Fig. 2 and Fig. 3 will have a slightly change, due to the fact that the neutrino energy is different. However the qualitatively result will be the same.

2.2 Anti-neutrino sources

Now we consider the case of a ${}^{90}\text{Sr} - {}^{90}\text{Y}$ anti-neutrino source. This source has been studied by a Moscow group [15] and its potential has been studied for the BOREXINO case [10].

We can make a similar analysis as in the case of the neutrino sources in the previous section. The main difference here, beside the interchange of g_L by g_R in

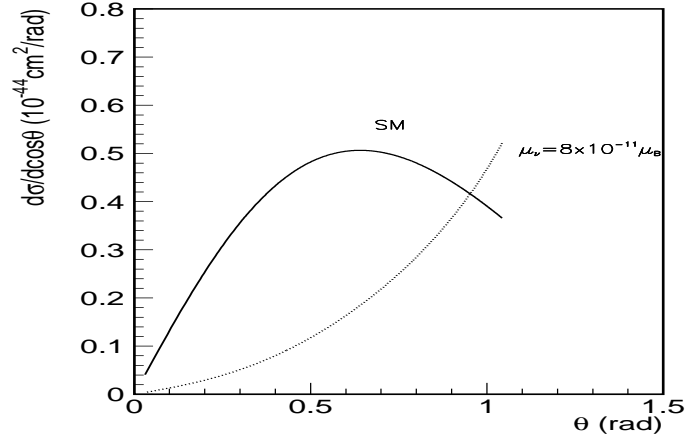


Figure 3: Differential cross section in terms of $\cos\theta$ for the SM case and for the case of a neutrino magnetic moment $\mu_\nu = 8 \times 10^{-11}$ in the case of a Cr source.

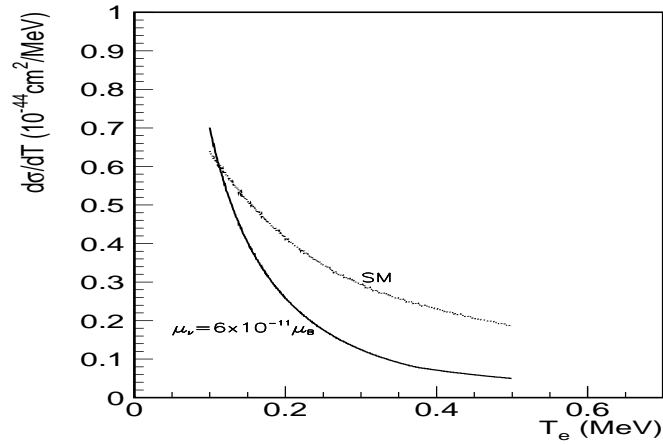


Figure 4: T-distribution of events for the SM case and for the case of a neutrino magnetic moment $\mu_\nu = 6 \times 10^{-11}$ for a $Sr - Y$ source. The angle θ has been integrated over.

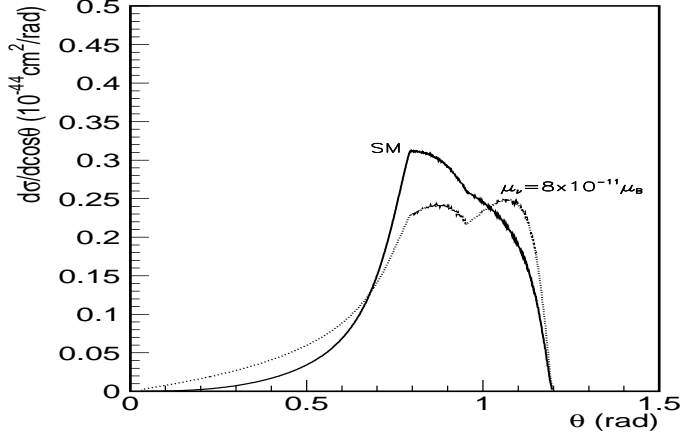


Figure 5: Angular distribution of events for the SM case and for the case of a neutrino magnetic moment $\mu_\nu = 6 \times 10^{-11}$. We consider a $Sr - Y$ source (Fig.1) and a threshold of $T_{th} = 100KeV$; the recoil energy is integrated, considering the cuts imposed by the threshold and the kinematical limits.

the differential cross section, is that we have an energy spectrum instead of a neutrino energy line. Therefore, we need integrate over the neutrino energy distribution. As we are interested in the angular distribution, it is more convenient to use Eq. (4) to make a change of variables in the integration. This has also been done in [14]. The result can be express as

$$\left\langle \frac{d\sigma}{dT} \right\rangle_{E_\nu} = \int \frac{d^2\sigma}{dT d(\cos\theta)} d(\cos\theta) = \int \Theta_{p. s.} f(T, \theta) \frac{d\sigma(T, \theta)}{dT} \frac{m_e p T}{(p \cos\theta - T)^2} d(\cos\theta) \quad (6)$$

or, if we are interested in the angular distribution

$$\left\langle \frac{d\sigma}{d(\cos\theta)} \right\rangle_{E_\nu} = \int \frac{d^2\sigma}{dT d(\cos\theta)} dT = \int \Theta_{p. s.} f(T, \theta) \frac{d\sigma(T, \theta)}{dT} \frac{m_e p T}{(p \cos\theta - T)^2} dT \quad (7)$$

In this equations $\Theta_{p. s.}$ accounts for the allowed phase space and $f(T, \theta) = f(E_\nu(T, \theta)) \equiv dn/dE_\nu$ is the neutrino energy spectrum as a function of T and θ .

We have computed the differential cross sections $d\sigma/dT$ and $d\sigma/d\cos\theta$ for an anti-neutrino energy spectrum given as shown in Fig. 1, normalized to one. In the case of $d\sigma/dT$ we have integrated Eq. (6) in the whole allowed θ range. For the case of the differential cross section $d\sigma/d\cos\theta$ we have integrated T in the range $.1MeV < T < 0.5MeV$, the energy range to which HELLAZ could be sensitive. The results are shown in Fig. 4 and Fig 5 both for the Standard Model case as well as for the case of a neutrino magnetic moment. Different values of the magnetic moment are shown in these figures. The kink in the distribution in Fig. 5 is due to the sharp decrease in the energy spectrum for $E_\nu > 0.5MeV$ (fig. 1).

Notice that, besides there is an additional contribution to the differential cross section, the shape is also different from that of the standard model. In particular the

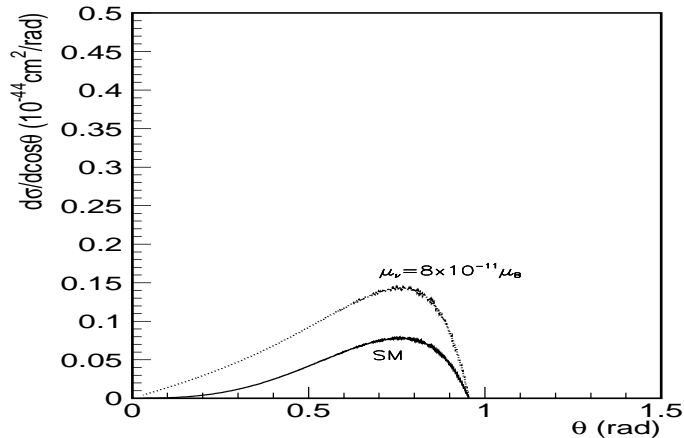


Figure 6: Same as in the previous figure but considering a hypothetical Sr source consisting only in the low energy part of the spectrum in Fig. 1 (neglecting the Y spectrum). Notice that the cross sections are smaller since we have cut part of the spectrum; the magnetic moment contribution becomes larger than the weak term since we restrict the spectrum to lower energies.

magnetic moment contribution is slightly bigger than the Standard Model one both for small angles and for big angles, meanwhile, in the intermediate region, the SM is bigger. However, the low values of the differential cross section in the small angle region, in comparison with other angles could make the analysis of this region more difficult. The case of the large angle region can be easily explained if we consider that, for minimum recoil electron energy the recoil angle is maximum, therefore, as the magnetic moment contribution increases at low T , it is natural to have a similar effect for large θ .

Besides the advantages that ANS have in general, this particular source seems to be interesting because the energy range of the spectrum that belongs to the ^{90}Sr has a peak in an energy range that is close to the kinematical zero that has been already discussed in the previous section. In order to illustrate the potential of this energy region we show in Fig. 6 the result that would be obtained for the ideal hypothetical case of a pure ^{90}Sr without any contaminant.

3 The NMM Signal and Recoil Angle Resolution

We now come back to the real $Sr - Y$ source. In this case one could try to optimise the best region in the $\theta - T$ plane on which the non-standard effect is maximum. In order to do this analysis let us consider the curves in the (T, θ) plane given by the condition

$$C = \frac{d\sigma^{mm}/dT}{d\sigma^W/dT} \quad (8)$$

This gives us the curves shown in Fig. 7. These are characterized by a given ratio

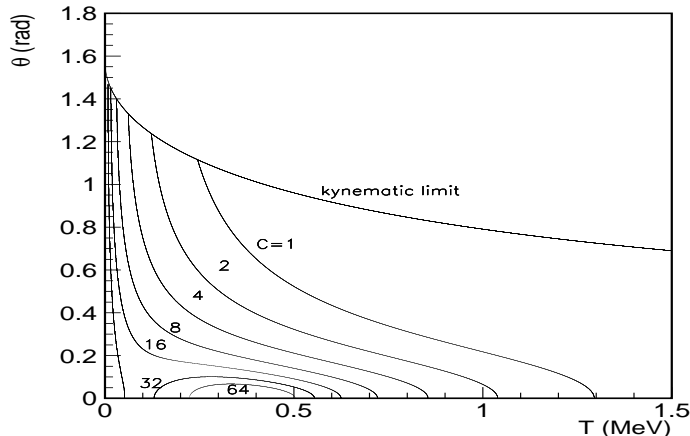


Figure 7: Curves of equal ratio $C \equiv \frac{d\sigma^{mm}}{dT} / \frac{d\sigma^W}{dT}$ for $\bar{\nu}_e$ and taking $\mu_\nu = 10^{-10} \mu_B$. Two are the effects which increase the ratio C : for low T the magnetic moment contribution becomes larger; for values of T and θ near the dynamical zero the weak term tends to cancel.

of the magnetic moment differential cross section to the SM one. Therefore, for $C=1$ we will get the curve where the magnetic moment signal is equal than the SM one, for $C=2$ the the magnetic moment signal is twice the SM one, and so on. The corresponding iso-curves are given in figure 7, for $\mu_\nu = 10^{-10} \mu_B$. In the figures the curves for $c = 1, 2, 4, 8, 32$ are shown; of course, for different selection of magnetic moments, the values of c in the same figure are scaled. For instance, taking $\mu_\nu = 10^{-11} \mu_B$, the curves shown in Fig. 4 would correspond to $c = 0.01, 0.02, 0.04, 0.08, 0.32$. It is also important to notice that, for any couple (θ, T) the neutrino energy is already fixed by the kinematics as can be seen from Eq. (4).

The effect of the dynamical zero on the iso-curves can be noticed specially in the cases of ratios $c = 32, 64$, where curves surrounding the position of the dynamical zero appear. This effect does not appear in the case of a neutrino source as can be seen in Fig. 8 where similar curves are shown for the case of $\nu_e - e$ scattering.

Given that the iso-curves (Fig. 7) reflect the presence of a favoured region for searching for a magnetic moment, thanks to the dynamical zero, it seems interesting to integrate the cross section over regions in the (T, θ) plane limited by the iso-curves. In this way, we are optimising the region of integration to look for magnetic moment.

Figure 9 shows the result of integrating the differential cross section given in Eq. (6) over T and θ in regions such that $d\sigma^{mm}/d\sigma^W > C$. A neutrino magnetic moment $\mu_\nu = 6 \times 10^{-11} \mu_B$ has been assumed. Of course, as the limiting ratio C is taken larger, the magnetic moment signal becomes larger than the SM one. However, the integral in this case is small. Note that if one integrates over the whole region ($C=0$) one can probe the complete cross section, but the value of NMM relative to SM decreases. Therefore it is interesting to study intermediate regions such as the region limited by $C = 0.7$, where the contribution of the neutrino magnetic moment is comparable with that of the weak interaction, although the statistics is a 30 % of the total one.

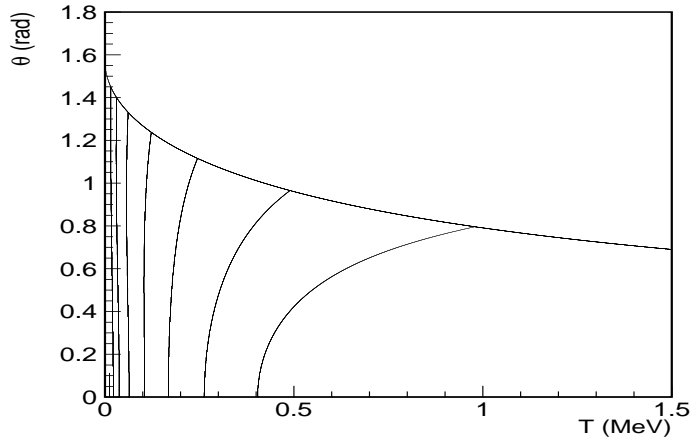


Figure 8: Curves of equal ratio $d\sigma^{mm}/d\sigma^W$ for ν_e . $\mu_\nu = 10^{-10}\mu_B$

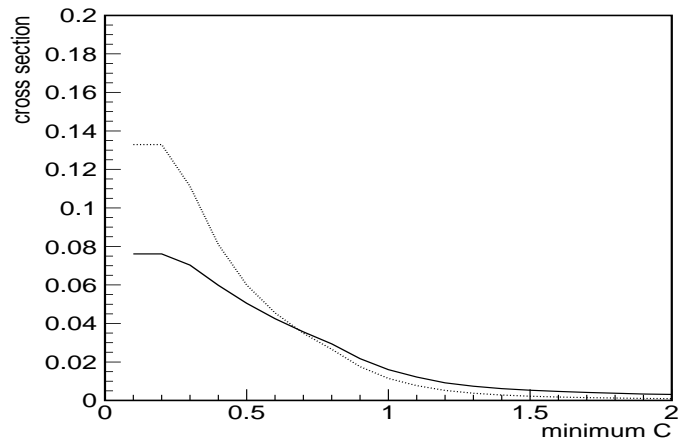


Figure 9: Weak and magnetic moment ($\mu_\nu = 6 \times 10^{-11}\mu_B$) integrated cross sections; we integrate both over angles θ and energies T . The region of integration is limited by the curves of equal ratio C ; the limiting value C is displayed in the horizontal axis; also, we consider a threshold for T : $T \geq T_{th} = 100 \text{ KeV}$. Both variables (T, θ) are also limited by the kinematics.

4 Discussion & Conclusions

We have discussed the potential of investigating neutrino-electron scattering as a probe of neutrino magnetic moment of the order $\mu_\nu \sim 10^{-11}\mu_B$ at low-threshold underground detectors with good angular and recoil electron energy resolution. We propose to do this using a number of artificial neutrino and anti-neutrino sources such as $^{51}\text{Cr}_{24}$ and $^{90}\text{Sr} - Y$. The neutrino flux is known to within a one percent accuracy, in contrast to the reactor case and one can reach lower neutrino energies. For the $^{90}\text{Sr} - Y$ source we have investigated the possible role of dynamical zeros in improving the sensitivity to the neutrino magnetic moment, with a negative result due to the poor statistics in this region. However, integrating over large kinematical regions, we estimated that the signal expected for a neutrino magnetic moment of $\mu_\nu = 6 \times 10^{-11}\mu_B$ will be comparable to that expected in the Standard Model and corresponds to a 30% enhancement in the total number of expected events. In order to provide a more reliable estimate of the sensitivities to the neutrino magnetic moment that can be reached in this kind of studies a dedicated experimental analysis will be necessary.

Acknowledgements

This work was supported by DGICYT grant PB95-1077, by Intas Project 96-0659 and by the EEC under the TMR contract ERBFMRX-CT96-0090. OGM was supported by SNI-México and by the grant CINVESTAV JIRA '99/08. VBS was supported by the RFFR grant 97-02-16501 and by Generalitat valenciana. We thank Tom Ypsilantis for discussions.

References

- [1] P. Vogel and J. Engel, Phys. Rev. **D39** 3378 (1989).
- [2] I. Barabanov *et al.*, Nucl. Phys. **B546** 19-32 (1999), hep-ph/9808297; O.G. Miranda, V. Semikoz and J. W. F. Valle, Phys. Rev. **D58**, 013007 (1998), hep-ph/9712215; O. G. Miranda, V. Semikoz and J. W. F. Valle, “Neutrino electron scattering as a probe of the electroweak gauge structure,” *In Valencia 1997, Beyond the standard model 340-344*, Ed. I. Antoniadis, L. Ibanez, J. W. F. Valle, World Scientific Publishing Co., 1998, ISBN 981-02-3638-7.
- [3] M. Moretti, C. Brogini and G. Fiorentini, “Physics beyond the standard model with a new reactor experiment,” Phys. Rev. **D57**, 4160 (1998).
- [4] E. Kh. Akhmedov hep-ph/9705451.
- [5] Cernyi *et. al.*, Phys. of At. Nuc. **57** 222 (1994).
- [6] MUNU Coll. C. Amsler *et. al.*, Nucl. Inst. and Meth. A369 115 (1997).
- [7] GALLEX Coll., *Phys. Lett.* **B342** 440 (1995); SAGE Coll., J. N. Abdurashitov, *et. al. Phys. Rav. Lett.* **23** 4708 (1996).
- [8] I. R. Barabanov *et. al.* Astro. Phys. **8** 67 (1997).
- [9] N. Ferrari, C. Fiorentini, B. Ricci, Phys. Lett. **B387** 427 (1996).
- [10] A. Ianni, D. Montanino, G. Scioscia hep-ex/9901012.
- [11] F. Arzarello, CERN-LAA 94-19.
- [12] T. Ypsilantis, private com.
- [13] J. Segura *et al.*, Phys. Rev. D49 1633 (1994).
- [14] J. Segura, Europhys. Jour. C (1998)
- [15] B. R. Bergelson, A. V. Davydov, Yu. N. Isaev, and V. N. Kornoukhov, Phys. of At. Nuc. **61** 1347 (1998).